Surface-Initiated Free Radical Polymerization of Polystyrene Micropatterns on a Self-Assembled Monolayer on Gold

Jinho Hyun and Ashutosh Chilkoti*

Department of Biomedical Engineering, Duke University, Box 90281, Durham, North Carolina 27708-0281

Received December 13, 2000; Revised Manuscript Received April 6, 2001

ABSTRACT: We describe the in situ synthesis of nanometer thick films of polystyrene (PS) on a self-assembled monolayer (SAM) on gold by surface-initiated free radical polymerization and further demonstrate that three-dimensional polymer structures with micrometer lateral resolution and nanometer vertical resolution can be fabricated by combining microcontact printing (μCP) with surface-initiated polymerization (SIP). We implemented SIP onto a COOH-terminated SAM on gold using a sequential approach to couple an amine-terminated free radical initiator to the terminal COOH groups presented by the SAM, followed by free radical polymerization of styrene. Each step of SIP was characterized by X-ray photoelectron spectroscopy and ellipsometry, and the PS film and micropattern were also characterized by atomic force microscopy. We typically obtained PS films with a thickness of 10−20 nm for a polymerization time of 12−24 h and with a root-mean-square roughness of ≤0.5 nm. PS micropatterns were also successfully fabricated by reactive μCP of the initiator onto a COOH-terminated SAM, followed by SIP of styrene. We also demonstrate two potential applications of SIP in biomaterials research: (1) label-free, real-time monitoring of protein adsorption on polymers by surface plasmon resonance (SPR) on nanometer thick homogeneous polymer films fabricated on a SAM on gold and (2) patterning cells on micropatterned polymers fabricated by combining μCP and SIP.

Introduction

We describe the in situ synthesis of nanometer thick films of polystyrene (PS) on a self-assembled monolayer (SAM) on gold by surface-initiated free radical polymerization and further demonstrate that three-dimensional polymer structures with micrometer lateral resolution and nanometer vertical resolution can be fabricated by combining microcontact printing (μCP) with surface-initiated polymerization (SIP).

Thin homogeneous polymer films and microstructures can be fabricated by many conventional methods such as spin-casting polymer solutions onto substrates, grafting polymers on surfaces by reaction from solution,[1] deposition of ionic polymers via electrostatic interactions,[2] and the growth of multilayers via covalent interactions.[3] Although these methods are useful, they have several limitations. Spin-casting polymers onto planar substrates is convenient and can yield homogeneous films ranging from tens of microns to well below a micron, but it is difficult to create polymer microstructures by spin-casting from solution. Grafting polymers from solution generally does not provide dense polymer brushes because of the steric barriers and unfavorable concentration gradient that limits diffusion of polymer molecules to the surface during the grafting process. The deposition of multilayer films via electrostatic interactions is limited to ionizable polymers.

In contrast, SIP can potentially circumvent these limitations. Because polymerization in SIP occurs from an initiator that is covalently immobilized on a surface, it should be possible to control both the thickness and graft density of the polymer. Furthermore, a wide variety of polymers can be synthesized by this methodology by appropriate choice of the polymerization chemistry; thin polymer films have been synthesized, in situ, on inorganic substrates using cationic,[4] anionic,[5] free radical,[6] living free radical,[7] Michael addition,[8] and ring-opening metathesis polymerization (ROMP).[9] Previous studies on SIP have focused on growing nanometer thick polymer films[4,5,6a,b,7a,8,9] and brushes on silica (or silicon dioxide) substrates.[6c−e,7b] These films have potential applications as soft alignment layers for liquid crystal cells,[6c] barrier layers for corrosion control, etch resists,[9] and matrices for capillary electrophoresis.[7a]

We are interested in developing complementary methods for SIP on SAMs on gold for the following reasons. First, SAMs on gold are well-defined and understood model organic interfaces.[10] Second, a wide variety of alkanethiols with different terminal functional groups are available, which enable the physical properties and chemical reactivity of the interface to be specified by choice of the appropriate alkanethiol or mixture of thiols.[11] Third, SAMs on gold have useful electrochemical[12] and optical properties (e.g., surface plasmon resonance (SPR)),[13] which can be directly exploited in biosensing. Finally, we are interested in nanoscale control of the topography of microstructured surfaces, because of its potential utility in the design of new surface architectures for fundamental studies on cell−surface interactions and biomaterials. SIP onto SAMs on gold should enable fabrication of micropatterned polymers with nanoscale control of topography, because of the diversity of soft lithography techniques (e.g., microcontact printing) that have been successfully applied to SAMs on gold.[14]

We therefore sought to implement a scheme for SIP onto a SAM on gold with the following attributes: (1) we wanted to develop an in situ, modular approach to polymer synthesis, which utilized commercially available reagents and stepwise, coupling reactions on SAMs on gold, and (2) we wished to develop a method that

* To whom correspondence should be addressed. Tel (919) 660-5373; FAX (919) 660-5362; E-mail chilkoti@duke.edu.

10.1021/ma002125u CCC: $20.00
Published on Web 06/27/2001

was compatible with soft lithography,[14] to allow the fabrication of micropatterned polymer films.

We implemented SIP onto a SAM on gold using a sequential approach to couple a free radical initiator to the surface, followed by polymerization of styrene. Each step of SIP was characterized by X-ray photoelectron spectroscopy (XPS), and polymer micropatterns formed by μCP of the initiator were characterized by XPS, imaging ellipsometry, and atomic force microscopy (AFM). We synthesized both 10−20 nm thick homogeneous films and patterned polymer films with micrometer lateral resolution and nanometer vertical resolution. Finally, we demonstrate two possible applications of SIP on SAMs on gold in biomaterials research: (1) label-free monitoring of protein adsorption on nanometer thick homogeneous polymer films by surface plasmon resonance (SPR) and (2) patterning of mammalian cells on a micropatterned polymer substrate, fabricated by combining reactive μCP and SIP.

Experimental Section

Materials. Styrene was purified using a DTR-7 column (Scientific Polymer Products), distilled in vacuo and stored in a freezer at −20 °C. 2,2′-Azobis(2-amidinopropane)dihydrochloride (Vazo56 WSP, DuPont), a water-soluble, amine-functionalized free radical initiator, was used as purchased. 11-Mercaptoundecanoic acid (MUA, 95%, Aldrich), 1-ethyl-3-(3-(dimethylamino)propyl)carbodiimide (EDAC, Aldrich), and pentafluorophenol (PFP, Aldrich) were used as purchased. Bovine serum albumine (BSA) was purchased from Sigma.

Preparation of Gold Substrates. The gold substrate for SIP was prepared by thermal evaporation of an adhesion layer of chromium (50 Å), followed by gold (450 Å for SPR or 2000 Å for all other measurements) onto a silicon wafer at 4×10^{-7} Torr. Before deposition, the silicon wafer was cleaned in a 5:1:1 (v/v) mixture of H_2O, H_2O_2, and NH_3 at 80 °C for 20 min.

Covalent Immobilization of Free Radical Initiator onto a Reactive SAM on Gold. The SAM of MUA was prepared by immersing a freshly prepared gold surface into an ethanol solution of 0.2 mM MUA overnight at room temperature. After formation of the SAM, the samples were washed with absolute ethanol, followed by ultrasonication in ethanol for 15 min, and dried under a stream of nitrogen. The terminal COOH groups in the MUA SAM were reacted with 0.1 M EDAC and 0.2 M PFP in ethanol for 20 min to convert the carboxylic acid groups to pentafluorophenyl esters. After reaction, the samples were rinsed with ethanol and dried under a stream of nitrogen. For synthesis of homogeneous PS films, the PFP-derivatized surface were reacted with a 10 mM solution of Vazo in methanol for 30 min. Alternatively, for fabrication of PS micropatterns, PFP-derivatized SAMs were microcontact printed with a plasma-oxidized PDMS stamp, which had been inked with a 10 mM solution of Vazo in methanol for 5 min. The surface was then washed with methanol and dried under a stream of nitrogen. Details on the fabrication of the PDMS stamps have been reported elsewhere.[15]

Surface-Initiated Polymerization of Polystyrene. SAMs on gold, presenting immobilized Vazo initiator on their surface, were introduced into a flask. A 1:2 v/v mixture of toluene and styrene was added to the flask, and the solution was degassed through at least five freeze−thaw cycles to remove oxygen from the monomer solution. Free radical polymerization was initiated by heating the solution to 65 °C. The polymerization time was typically in the range 12−24 h, and the reaction time is reported in the text or in figure captions, where relevant. After polymerization, the samples were Soxhlet extracted in toluene for at least 12 h to remove physisorbed polymer originating from solution polymerization of styrene.

X-ray Photoelectron Spectroscopy. XPS was performed on a SSX-100 spectrometer (Surface Science Inc., Mountain View, CA) equipped with a monochromatized Al Kα X-ray source, a hemispherical electron analyzer, and a low-energy electron flood gun for charge compensation. Samples were typically introduced into a preparation chamber, which was maintained at a pressure of 10^{-4} Torr, and then transferred into the analysis chamber, which was typically maintained at 10^{-8} Torr. The samples were analyzed at 15°, 35°, or 55° takeoff angle, defined as the angle between the sample plane and the entrance axis of the hemispherical analyzer. The typical X-ray spot size was 1000 μm. Survey scan spectra were acquired from 0 to 1000 eV for elemental composition, and high-resolution spectra of the C_{1s} core level were acquired from 279 to 299 eV.

Ellipsometry. A manual null ellipsometer, built in-house, was used for ellipsometric measurements. A He−Ne laser (632.8 nm, Melles Griot) incident at an angle of 68.25° was used as the light source for intensity as well as for imaging ellipsometry. Polarizer angles were determined with a precision of 0.01°, and the intensity was measured with a lock-in amplifier (Princeton Applied Research, Princeton, NJ). Ellipsometric constants of the substrate were measured before and after modification. For imaging ellipsometry, two lenses were inserted into the output beam, and the detector was replaced with a CCD camera with fixed gain and black level (Dage-MTI) connected to a computer for digital acquisition of images. The magnification was ∼9 ×. To obtain the ellipsometric constants of a micropatterned substrate in imaging ellipsometry, the polarizer and analyzer angles were adjusted to minimize the signal from either the patterned region or background in separate measurements. The polarizer and analyzer angles obtained from each set of measurements were used to independently calculate the thickness of each layer. The thickness of the SAM and homogeneous PS films and micropatterns were calculated using a parallel slab model[16] with assumed refractive indices of 1.00 for air, 1.5 for the SAM,[17] and 1.59 for the polymer.[18]

Surface Plasmon Resonance. The BiacoreX instrument (Biacore AB, Sweden) was used for surface plasmon resonance (SPR) studies. Typically, polymers or SAMs were prepared on a gold-coated glass coverslip (450 Å gold thickness) and mounted in an empty Biacore sensor cartridge using water-insoluble, double-sided sticky tape (3M Corp.). The sensor cartridge was docked into the BiacoreX instrument and checked for the absence of leaks and baseline drift. SPR measurement of BSA adsorption in PBS was performed at a constant flow rate of 10 μL/min for 5 min at different concentrations of BSA in solution. After adsorption, desorption of the protein from the polymer surface was monitored by SPR at a flow rate of 10 μL/min of PBS for 5 min.

Atomic Force Microscopy. Contact mode AFM imaging was performed on a MultiMode SPM (Digital Instruments) in air using a standard silicon nitride tip (Nanoprobe SPM, Digital Instruments) with a spring constant of 0.12 N/m at a scan rate of 3.05 Hz.

Cell Adhesion Measurement. FADU cells, a human cell line from a hypopharyngeal carcinoma, were grown in Dulbecco's modified eagle medium (DMEM, Gibco Laboratories) supplemented with 10% fetal bovine serum (FBS, Gibco Laboratories), 100 units/mL penicillin, 100 mg/mL streptomycin, and 7.5 mM HEPES at 37 °C in 5% CO_2. Cells were removed from the tissue culture flask by brief treatment (∼2 min) with 0.05% trypsin−EDTA (Gibco Laboratories) and plated on patterned samples or controls at a density of 10^6 cells/mL in DMEM supplemented with 10% serum. Cells were incubated at 37 °C for 90 min. Nonadherent cells were washed away, and adherent cells were fixed for 10 min in 2% (w/v) paraformaldehyde, incubated with a 2 mM solution of FM1-43, a fluorescent lipophilic dye (Molecular Probes, Eugene, OR) in DMEM to label the plasma membrane, and then washed in growth medium. Cells were then visualized by epifluorescence microscopy using fluorescence optical filters.

Results and Discussion

We implemented SIP onto a SAM on gold using a sequential approach to couple a free radical initiator to

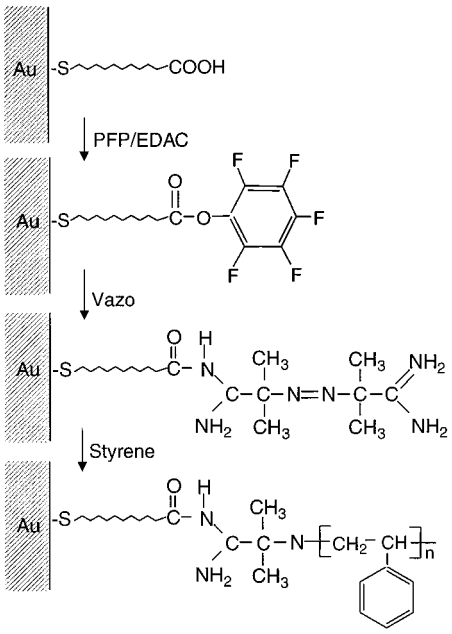

Figure 1. Schematic of surface-initiated free radical polymerization of styrene on gold.

the surface followed by polymerization of styrene, as follows (Figure 1): (1) a SAM, presenting terminal carboxylic acid groups, was formed by self-assembly of MUA from solution onto gold; (2) the terminal COOH group in the MUA SAM was converted to pentafluorophenyl ester by reaction with PFP/EDAC;[19] (3) a commercially available, amine-terminated free radical initiator, Vazo, was reacted with the pentafluorophenyl ester, either from solution or by spatially resolved transfer using an elastomeric stamp inked with the initiator; and (4) styrene was polymerized at the surface by free radical polymerization. We chose to polymerize styrene by SIP, because its free radical polymerization on a surface has been previously demonstrated on silica.[6a,b] Furthermore, the absence of oxygen in polystyrene (PS) and its aromatic substituent facilitates its surface characterization by XPS.

Characterization of Homogeneous PS Films Synthesized by SIP. We fabricated PS films and characterized the fabrication process by ellipsometry, XPS, and AFM. XPS enabled unambiguous surface characterization because unique elements were introduced at each step in the SIP of styrene. First, the gold surface was modified by solution self-assembly of a MUA SAM, which resulted in a 1.5 nm thick film on gold as measured by ellipsometry. XPS of the MUA SAM on gold showed the introduction of a unique sulfur S_{2p} signal at 162 eV and an O_{1s} signal at 533 eV (Figure 2, spectrum I). The experimental atomic O/C ratio of 0.185 determined by XPS is close to the calculated ratio from the stoichiometry of the SAM, suggesting the formation of a SAM of MUA without significant organic contamination or defects. Au peaks with significant intensity (Figure 2, spectrum I; Au/C ratio of 0.3 in Table 1) were also observed, consistent with the fact that the 1.5 nm thickness of the MUA SAM, measured by ellipsometry, is smaller than the 5−8 nm sampling depth of XPS at a takeoff angle of 55° for organic overlayers.[20−22]

One concern in the implementation of SIP on gold was the ability of the MUA SAM to resist organic solvents at the temperatures typically used in free radical polymerization. We therefore examined the thermal

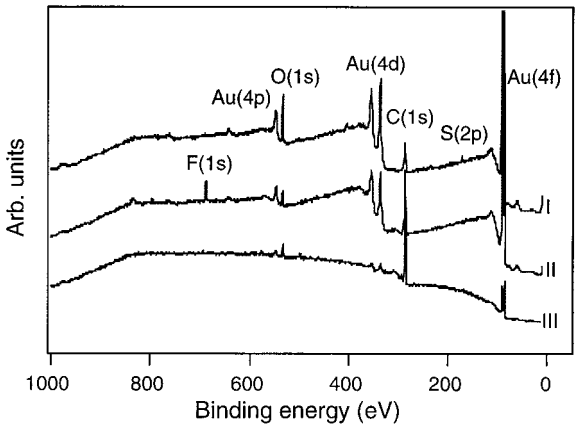

Figure 2. XPS survey scan of the different modification steps in SIP on gold: (I) MUA SAM on gold, (II) PFP derivatization of MUA SAM, (III) formation of a PS film by SIP (12 h polymerization time; 8 nm ellipsometric thickness).

Table 1. Elemental Analysis of Derivatized Surfaces by XPS

	measured				calculated			
	O/C	F/C	N/C	Au/C	O/C	F/C	N/C	Au/C
thiol	0.185	0	0	0.300	0.182	0	0	
PFP	0.131	0.126	0	0.246	0.118	0.294	0	
PS	0.074	0	0	0.027	100	0	0	0

stability of the MUA SAM on gold upon immersion in toluene at 65 °C for 12−24 h, solution conditions that were typically used in SIP. The atomic O/C and S/C ratio of the MUA SAM were experimentally indistinguishable from the control SAM, which had not been incubated in toluene at elevated temperature (results not shown).

Next, the terminal COOH group in the MUA SAM was activated by reaction with PFP (Figure 1). We chose PFP to activate the COOH group in PET−COOH, because previous reports have suggested that pentafluorophenyl esters are significantly more reactive than the more commonly used *N*-hydroxysuccinimide ester.[19] Fluorine was introduced as a new element upon derivatization of the MUA SAM on gold with PFP (Figure 2, spectrum II). The experimental F/C ratio of 0.126 after derivatization of the MUA SAM with PFP is significantly lower than the calculated ratio of 0.294 (Table 1), assuming complete derivatization of the COOH group, and indicates that only ∼25% of the COOH groups were derivatized with PFP. This finding is consistent with the expected steric barrier to coupling of PFP to the COOH group, due to the larger size of the PFP substituent compared to the COOH moiety. This result also suggests that conversion of the COOH group in the MUA SAM to pentafluorophenyl ester could be optimized by diluting the MUA SAM with a diluent alkanethiol presenting an unreactive functional group (e.g., CH_3, OH) in order to maximize the accessibility of the COOH group to PFP. After immobilization of the Vazo initiator, a 0.6 nm increase in thickness was measured by ellipsometry relative to the MUA SAM. We attempted to analyze the Vazo-modified SAMs by XPS but obtained irreproducible results, which we speculate are caused by side reactions of the thermally labile, reactive initiator upon prolonged exposure to air and ambient water vapor prior to XPS analysis and also due to electron beam damage during analysis.

The Vazo-modified SAM was incubated with styrene, and the solution was heated to 65 °C to initiate free

Table 2. Variable Takeoff Angle XPS Results for a Homogeneous PS Film Fabricated by SIP on an MUA SAM on Gold

	atomic percent (%)		
takeoff angle (deg)	C	O	Au
15	91.41	4.17	4.12
35	49.94	5.81	14.25
55	69.71	7.42	22.87

[a] Polymerization time = 6 h.

radical polymerization of styrene from the surface of the SAM. The polymerization was typically carried out for 12 or 24 h, and the thickness of the polymer overlayer ranged from 8−10 nm (12 h) to 15−20 nm (24 h) as measured by ellipsometry after extensive extraction of the samples in toluene. The survey scan spectrum of the surface-initiated polymerization of styrene is shown in Figure 2 (spectrum III). A dominant C_{1s} signal and smaller Au_{4f} and O_{1s} peaks were observed in the spectrum. The dramatic decrease in the O/C and Au/C ratio compared to the PFP-derivatized SAM indicated the formation of a PS overlayer on the substrate (Table 1), whose thickness is close to the 7 nm XPS sampling depth for PS at a 55° takeoff angle.[23] The XPS results are in reasonable agreement with the 8 nm thickness of the film, independently measured by ellipsometry.

Partial coverage of the substrate by PS and the oxidation of the surface PS layer are alternative possibilities that could account for the observed O_{1s} and Au_{4f} signals in the survey scan spectrum of PS synthesized by SIP. We examined these possibilities by performing variable takeoff angle XPS on a PS overlayer synthesized by SIP on the SAM (Table 2). To examine the distribution of elements as a function of XPS sampling depth, we chose a shorter 6 h polymerization time for this sample. The Au/C ratio and the O/C ratio increased as a function of takeoff angle. These results indicate a thin overlayer in which the Au atoms as well as the oxygen-containing moieties are preferentially localized in the subsurface region. The increased O/C ratio with increasing XPS takeoff angle is consistent with the spatial distribution of the COOH groups in the SAM, which are buried below the PS overlayer formed by SIP of styrene. These results do not, however, rule out partial coverage of PS over the 1 mm^2 area interrogated by XPS. The increase in the O/C and Au/C atomic ratio with increasing XPS sampling depth does, however, rule out the possibility of significant surface contamination by oxygen-containing species or postpolymerization oxidation of the PS overlayer.

The stepwise modification of gold and subsequent polymerization by SIP was also studied by high-resolution XPS of the C_{1s} core level (Figure 3), and the curve-fitting results for each C_{1s} spectrum[24,25] are summarized in Table 3. A peak at 289 eV in the spectrum of the MUA SAM on gold is consistent with the presence of the terminal COOH group in the SAM (Figure 3A), though the CH_x + C−S:COOH ratio of 4.9 is somewhat lower than the stoichiometric ratio of 10 (Table 2). Derivatization of the COOH groups by PFP results in loss in the intensity of the COOH moiety and the appearance of a shoulder at lower BE (Figure 3B). Deconvolution of the spectrum suggested a peak at 288 eV, which could be assigned to the C−F species. This peak accounted for ∼12% of the overall peak intensity of the C_{1s} spectral envelope (Table 3), which is consistent with the 10% peak intensity calculated from the stoichiometry of the reaction, assuming 25% conversion of the COOH group to pentafluorophenyl ester, as shown by the XPS survey scan of the PFP-derivatized MUA SAM on gold.

The C_{1s} spectrum of the surface after SIP of styrene provided clear evidence that the polymerization of styrene was successful (Figure 3C). A symmetric peak at 285 eV could be assigned to the CH_x species, and a secondary peak with an overall intensity ∼5% that of the CH_x peak was clearly observed at 292 eV (Table 3). The binding energy (BE) of this peak, its significantly lower intensity relative to the peak at 285 eV, and its full width at half-maximum (fwhm) of ∼1.7 eV enable assignment of this peak to a $\pi \rightarrow \pi^*$ shake-up satellite from the aromatic substituent of PS.[26]

Although the XPS results (Figures 2 and 3) are consistent with stepwise derivatization and surface-initiated polymerization from the immobilized free radical initiator, we performed additional experiments to verify that the attachment of initiator and polymerization of styrene proceeded as shown in Figure 1. In independent control experiments, we carried out the SIP of styrene by omitting either activation of the COOH groups in the MUA SAM by PFP/EDAC or attachment of the free radical initiator. For both controls, XPS showed the absence of a PS overlayer, both in the survey scan spectrum and by the absence of a symmetric C_{1s} envelope and $\pi \rightarrow \pi^*$ shake-up satellite in the high-resolution C_{1s} spectrum (results not shown).

We also examined the SIP of styrene by contact mode AFM in air (Figure 4). AFM imaging showed that polymerization of styrene significantly altered the topography of the gold surface. (Figure 4A). AFM images of PS, synthesized by SIP on gold, showed a homogeneous layer over areas of several hundred μm^2 (Figure 4B), with a root-mean-square (rms) roughness of <0.5 nm over a 2 μm × 2 μm scan area, which is significantly smaller than the 5 nm rms roughness of polycrystalline gold over the same area. The surface topography measured by AFM of the PS films on gold reported here, and in a previous study on silicon oxide,[6] were very similar, with rms roughness of <1 nm and peak-to-valley height differences of <3 nm.

Although there are several experimental differences between this study and that of Prucker et al. which preclude direct comparison, in general the thickness of PS films obtained in this study (e.g., ∼10 nm for a polymerization time of 12 h) was significantly smaller than those obtained by Prucker et al. on silicon oxide for the same polymerization time (∼40 nm).[6] Experimental differences between the two systems, such as the surface concentration of immobilized initiator and the polymerization temperature, may account for these results. An alternative explanation of the observed differences in the film thickness originating from the lower thermal stability of alkanethiol SAMs would require SIP to be performed on the two substrates under identical experimental conditions. While this paper was under review, Huang et al. reported similar results for SIP of styrene on a MUA SAM on gold.[27] They suggest that three factors might account for the smaller film thickness observed on SAM on gold as compared to SAMs on silicon oxide or aluminum. These are (1) partial, thermally induced desorption of initiator-functionalized monolayers on gold under typical thermally initiated polymerization conditions, (2) desorbed thiols may serve as chain transfer agents which would termi-

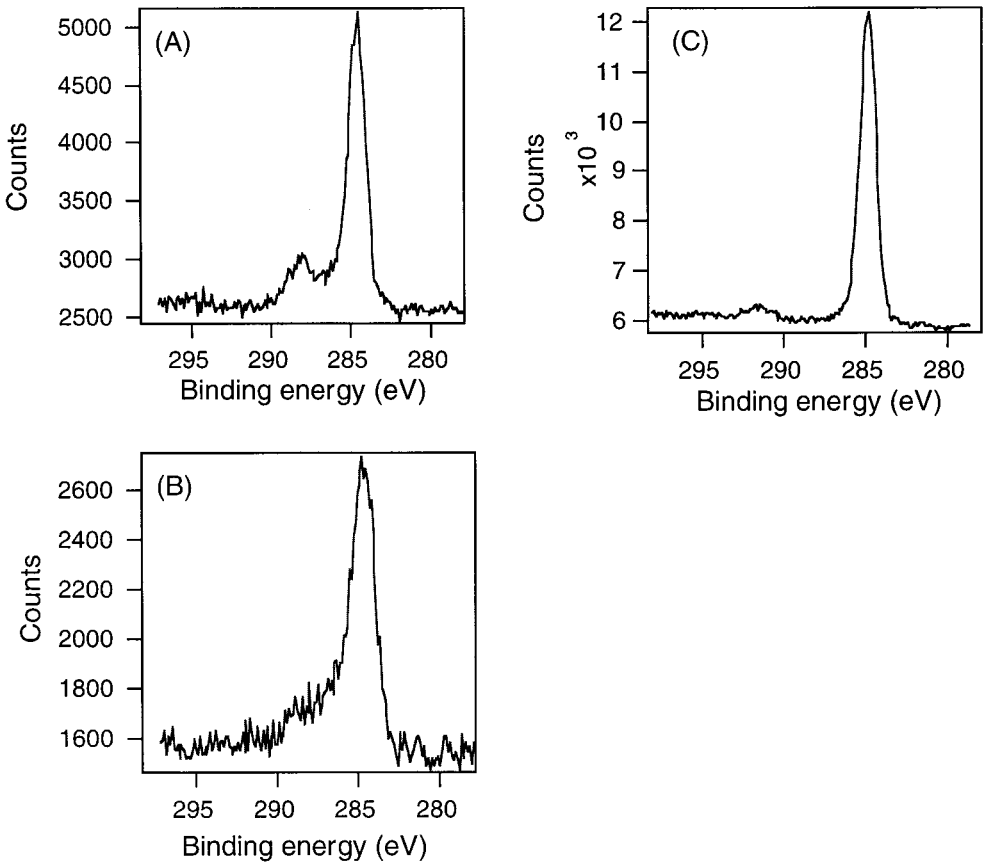

Figure 3. XPS C_{1s} spectrum at each stage of SIP of styrene on gold: (A) MUA SAM on gold, (B) PFP-derivatized MUA SAM on gold, (C) PS film.

Table 3. XPS C_{1s} Component Peaks of Modified Gold Surfaces at Different Stages of SIP of Styrene on Gold

functional group	C_{1s} BE (eV)	C_{1s} component (%)		
		MUA SAM	PFP	PS
C−C	285.0	69.1 (81.8)	73.3 (72.0)	95.0 (90.0)
C−S	285.4	13.9 (9.1)	(8.0)	
C−NH_x	286.0			
C−O	286.5		9.5 (2.0)	
C−F	287.9		11.5 (10.0)	
NH_x−C=O	288.1			
O−C=O	289.0	17.0 (9.1)	5.7 (8.0)	
$\pi-\pi^*$	292.0			5.0 (10.0)

[a] Styrene was polymerized for 12 h by free radical polymerization and an 8 nm PS film was obtained, as measured by ellipsometry. Parentheses are calculated values.

nate polymer growth from the surface, and (3) radicals in solution or on the surface could accelerate desorption of thiols or their oxidation products.

Protein Adsorption on Homogeneous Polymer Films Fabricated by SIP. We are specifically interested in using SIP to fabricate thin polymer films for two biomedical applications. First, thin homogeneous polymer films that are directly polymerized onto SAMs on gold are likely to be more robust substrates for optical biosensing (e.g., SPR) than SAMs on gold. Second, thin polymeric films synthesized by SIP on gold are useful from a biomaterials perspective, because a large number of free radical polymers such as polystyrene, polyacrylates, and polymethacrylates are commonly used in tissue culture and as biomaterials.[28] The adsorption behavior of proteins from serum or blood onto a biomaterial is an important interfacial property of interest. The formation of nanoscale thickness films of polymers on a gold substrate by SIP should enable protein adsorption to be studied by SPR reflectometry in an aqueous environment of interest.

In principle, studying the adsorption of proteins onto polymers by SPR is attractive because, unlike current methods to study protein adsorption such as radiolabeling and ELISA, SPR does not require extrinsic labels and also enables adsorption kinetics to be monitored in real time.[29] SPR, however, requires the use of reflective gold or silver substrates (e.g., 450 Å gold deposited on glass), and the material of interest has to be deposited onto the gold substrate. The critical challenges in fabricating polymer films on gold (or silver) for use in adsorption (or binding) studies by SPR are twofold: Because surface plasmons decay exponentially with distance from the metal film,[30] the polymer film on gold should be thin enough so that the subsequent adsorption of a protein onto the polymer film can be detected by SPR with high analytical sensitivity. Second, the film should be uniform and defect free over at least several hundred micrometers to ensure that the interaction between the protein and the polymer surface are interrogated by SPR rather than with the underlying SAM on gold.

Davies et al. have previously shown that SPR can be used to monitor the adsorption of proteins on polymers deposited onto silver by solution casting.[31] SIP provides an alternative approach to the fabrication of nanometer thick homogeneous polymer films that are suitable substrates for adsorption or binding studies by SPR. Figure 5A shows real-time sensorgrams[32] of BSA adsorption from solution onto a gold SPR chip coated with a 20 nm thick PS film for a range of BSA solution

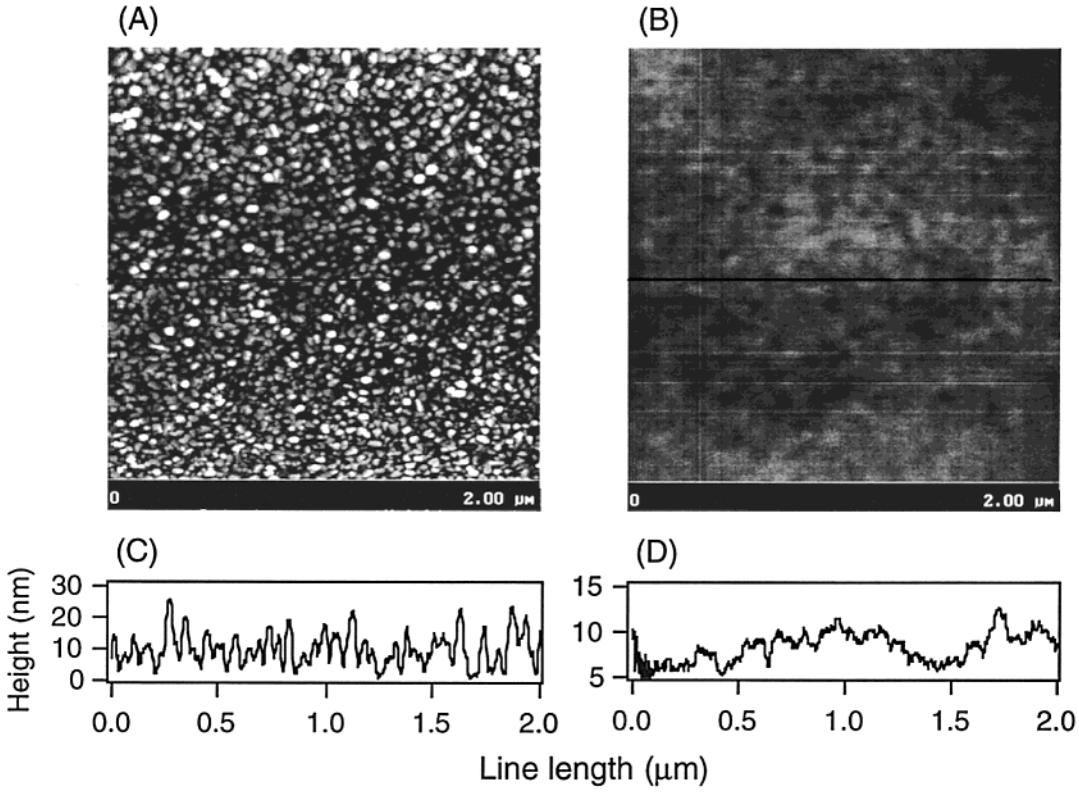

Figure 4. Contact mode AFM images of (A) gold, (B) PS synthesized by SIP on a MUA SAM on gold (24 h polymerization time; 20 nm ellipsometric thickness), (C) line profile across the AFM image of the gold surface in (A), and (D) line profile across the AFM image of the PS film in (B).

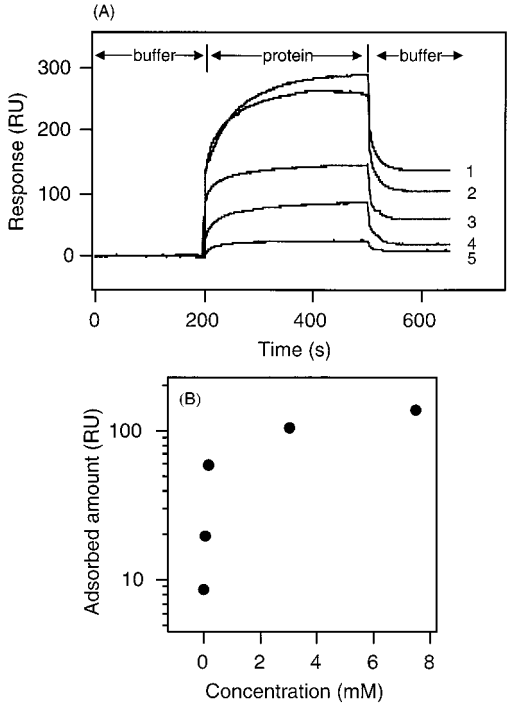

Figure 5. SPR measurement of BSA adsorption on a PS film on gold synthesized by SIP. (A) Sensorgrams of BSA adsorption and desorption from a 20 nm thick PS film prepared by SIP at different concentrations of BSA: (1) 7.5 mM, (2) 3.0 mM, (3) 150 μM, (4) 15 μM, (5) 1.5 μM. (B) Steady-state adsorption of BSA on PS in resonance units (RU) as a function of BSA solution concentration.

concentrations. The sensorgram is a plot of the change in the resonance signal as a function of time. The BSA solution was injected in a pulse from 200 to 500 s, and protein adsorption on the PS surface was followed by observing the change in resonance signal as a function of time. The protein bound to the polymer surface during injection and loosely bound protein dissociated when the protein was replaced with buffer. The amount of adsorbed protein on the polymer surface was obtained from the difference of the steady-state SPR response between the association and dissociation parts of the sensorgram. The SPR sensorgrams (Figure 5A) as well as the steady-state amount of BSA adsorbed (Figure 5B) as a function of BSA solution concentration show that the minimum detection limit for BSA adsorption by SPR is ~1.0 μM. Although the detection limit for protein adsorption on polymers by SPR is comparatively higher than that obtained by using radiolabeled proteins, SPR has the important advantages of being a label-free technique, enabling adsorption kinetics to be quantified in real time, as well as quantitation of the total protein adsorbed on a surface from complex protein mixtures such as serum and plasma.

Fabrication and Characterization of Micropatterned PS Films. Combining SIP with soft lithography is attractive for applications that require polymer structures with micron-scale lateral and nanometer-scale vertical resolution. We are specifically interested in fabricating polymeric structures with these dimensions as substrates for cell interaction studies. To microfabricate PS patterns by SIP, a plasma-oxidized PDMS stamp with 40 μm wide lines was inked with a solution of the initiator in methanol and brought into conformal contact with the surface of a PFP-derivatized MUA SAM on gold. This resulted in spatially resolved transfer and reaction of the initiator with the surface. A film of PS was then grown in the regions of the surface containing immobilized initiator by SIP and imaged by

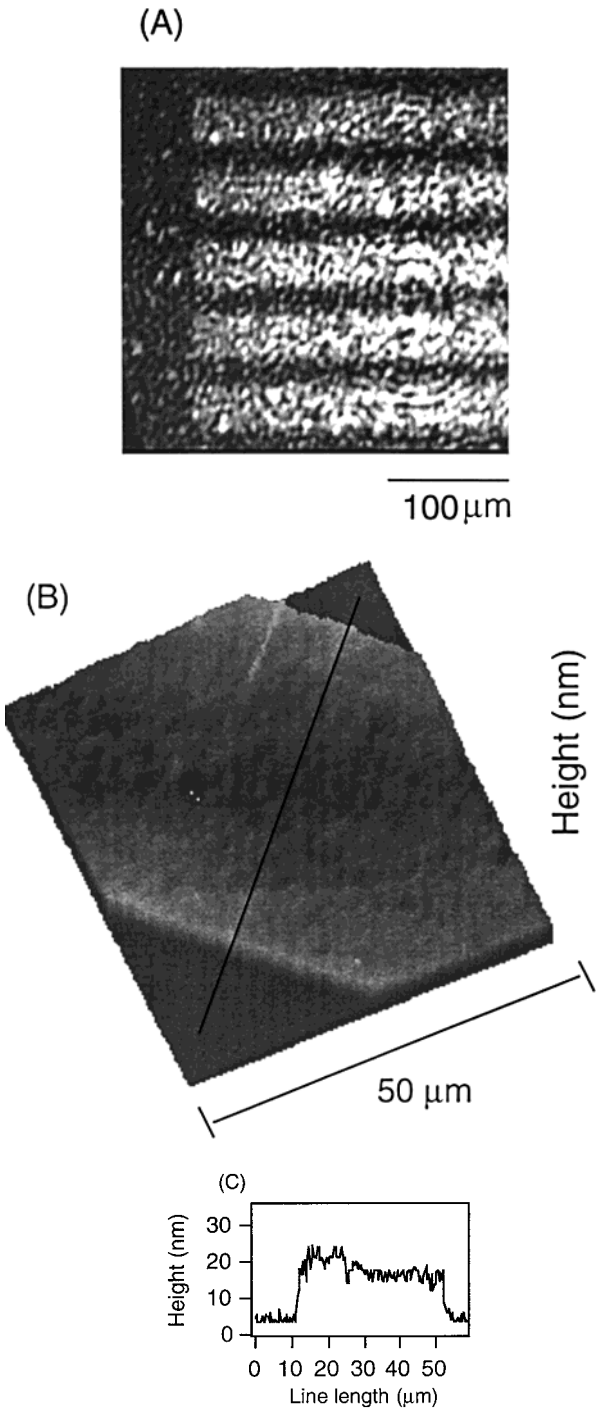

Figure 6. PS micropatterns fabricated by SIP of styrene by reactive μCP of an amine-terminated free radical initiator onto a MUA SAM on gold, followed by SIP of styrene: (A) ellipsometric image (12 h polymerization time; 8 nm ellipsometric thickness of micropatterned PS features); (B) AFM image (24 h polymerization time; 20 nm height); (C) line profile across the image in (B).

AFM and ellipsometry (Figure 6). Imaging ellipsometry is an attractive method to image topographical variations on a substrate because it is a nondestructive method that does not require extrinsic chromophores and allows relatively large areas of the surface to be imaged. Imaging ellipsometry is also a quantitative method because it provides the coverage density or an effective thickness of the micropatterned regions.[33]

A representative ellipsometric image of a PS pattern fabricated by reactive μCP of the initiator using a PDMS stamp with 40 μm wide lines, and a polymerization time of 12 h at 65 °C, is shown in Figure 6A. Imaging ellipsometry showed that the micropatterned PS was spatially localized to the regions that were in contact with the surface of the stamp (Figure 6A). Quantitative analysis of the image showed that the thickness of the polymer layer was ~8 nm. A contact mode AFM image of a sample fabricated by SIP of PS from a SAM presenting patterned Vazo groups is shown in Figure 6B. The thickness of the polymer layer was determined to be ~20 nm by measuring the step height by AFM (Figure 6C), which is consistent with the longer, 24 h polymerization time used to fabricate this sample.

Application of SIP to Pattern Cells on Substrates. The patterning of cells onto surfaces is of increasing interest in the design of biomaterials, cell-based sensors, and combinatorial library screening. A number of methods have been developed to pattern cells onto solid substrates, which are derived either from photolithography[34] or soft lithography.[14] In particular, a number of soft lithography patterning methods such as microcontact printing[35] patterning using microfluidic flow channels,[36] laminar flow patterning,[37] and elastomeric stencils[38] have been developed to pattern cells onto surfaces.

We believe that a useful application of SIP is in the design of new surface architectures to modulate cell−surface interactions by engineering the topography and chemistry of a surface. We therefore explored the feasibility of fabricating micropatterned PS films by combining SIP with μCP and performed preliminary studies of the interaction of the microfabricated polymer structures with mammalian cells.

We examined the attachment of a mammalian cell line to a patterned surface which comprised of 40 μm wide micropatterned PS features with ~20 nm high walls, fabricated by SIP onto a MUA SAM on gold. The interfeature spacing which comprised the MUA SAM was 35 μm. Figure 7 shows an epifluorescence image of cells attached to micropatterned PS features on a MUA SAM. As shown in Figure 7A, the cells display a significant spatial preference in their attachment to the surface of the micropatterned substrate. Control experiments, where the cells were independently seeded onto a homogeneous MUA SAM or a PS film (parts B and C of Figure 7, respectively) showed that the cells prefer to attach to the hydrophilic MUA surface rather than the hydrophobic PS surface. These results clearly indicate that the cells attached to the MUA SAM between the PS walls on the substrate on the micropatterned PS substrate (Figure 7A). The attachment of cells to the MUA monolayer, as opposed to the PS features, is consistent with previous work by Leggett and colleagues, who have shown that in serum certain mammalian cell lines such as fibroblasts show a marked preference for COOH-functionalized surfaces.[39] These initial results show that the combination of nanoscale walls and a favorable surface chemistry largely confines cells to the COOH tracks on the surface.

In its ability to create three-dimensional structures with micron-scale lateral and nanometer-scale vertical resolution, SIP is complementary to other soft lithography patterning methods.[35−38] In particular, SIP should allow independent control of topographical and chemical features. For example, SIP in combination with μCP should allow independent control of the width of the patterned polymer features as well as their height at

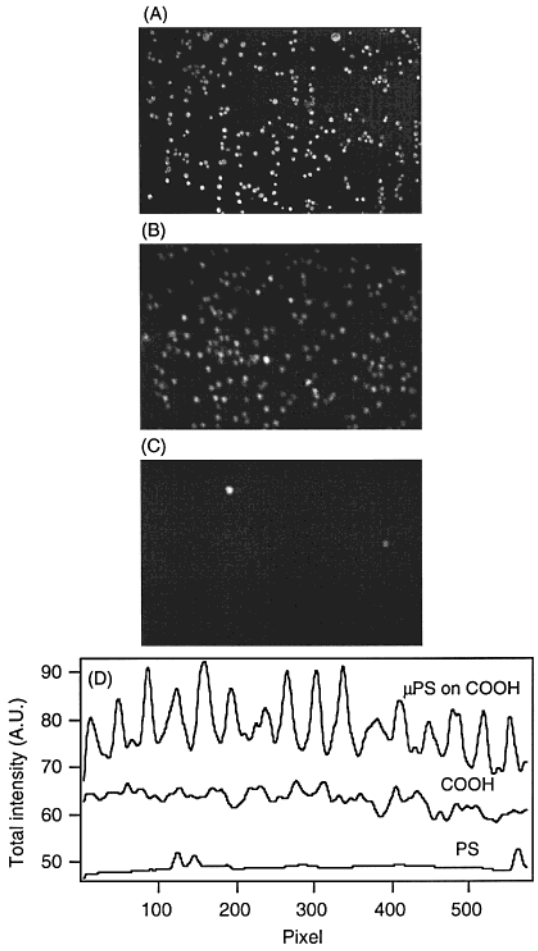

Figure 7. Epifluorescence images of cell attachment on (A) PS microstructures (width 40 μm, height 21 nm; interfeature spacing 35 μm) fabricated by reactive μCP of free radical initiator followed by SIP of styrene (24 h polymerization time) on a MUA SAM on gold, (B) MUA SAM on gold, (C) spin-cast PS film on gold, and (D) integrated fluorescence intensity as a function of horizontal pixels for panels A−C.

the nanoscale. SIP should also enable chemistry and topography to be independently controlled: after SIP of a monomer, the background could be filled in with the same or different polymer by a subsequent round of SIP. Surface structures fabricated by these methods will also facilitate investigation the role of surface chemistry and nanoscale topography in controlling cell adhesion, migration, and proliferation, with implications to the design of textured biomaterials and tissue engineering scaffolds.

In conclusion, we believe that SIP combined with soft lithography is a useful method to fabricate polymer surface structures with independent control of lateral and vertical resolution at size scales ranging from a few nanometers to the micrometer scale as well as flexibility in surface chemistry. Achieving this goal, however, will require further elucidation of the factors involved in controlling the stability of SAMs during surface-initiated polymerization on gold.

Acknowledgment. We thank Prof. Gabriel Lopez (University of New Mexico, Albuquerque, NM) for sharing a recently submitted manuscript on the in situ polymerization of poly(*N*-isopropylacrylamide) as well as for useful discussions. We thank Harry Sugg and Dr. Andrea Liebmann-Vinson (Becton-Dickinson Technologies) for XPS analysis and Dr. Drazen Raucher (Duke University) for performing the cell culture studies. The AFM instrumentation used in this study was provided by a multiuser instrumentation grant (DBI-96-04785)) from the National Science Foundation and an institutional development grant (9703-ID1002) from the North Carolina Biotechnology Center.

References and Notes

(1) Fery, N.; Laible, R.; Hamann, K. *Angew. Makromol. Chem.* **1973**, *34*, 81−109. Laible, R.; Hamann, K. *Adv. Colloid Interface Sci.* **1980**, *13*, 65−99. Bridger, K.; Vincent, B. *Eur. Polym. J.* **1980**, *16*, 1017−1021. BenOuada, H.; Hommel, H.; Legrand, A. P.; Balard, H.; Papirer, E. *J. Colloid Interface Sci.* **1988**, *122*, 441−449. Tsubokawa, N.; Hosoya, M.; Yanadori, K.; Sone, Y. *J. Macromol. Sci., Chem.* **1990**, *A27*, 445−457. Kurth, D. G.; Broeker, G.; Kubiak, C. P.; Bein, T. *Chem. Mater.* **1994**, *6*, 2143−2150. Bruening, M. L.; Zhou, Y.; Aguilar, G.; Agee, R.; Bergbreiter, D. E.; Crooks, R. M. *Langmuir* **1997**, *13*, 770−778.

(2) Decher, G. *Science* **1997**, *277*, 1232−1237. Decher, G.; Hong, J. D.; Schmitt, J. *Thin Solid Films* **1992**, *210*, 831−835. Cheung, J. H.; Fou, A. F.; Rubner, M. F. *Thin Solid Films* **1994**, *244*, 985−989. Hammond, P. T.; Whitesides, G. M. *Macromolecules* **1995**, *28*, 7569−7571. Lasshewsky, A.; Mayer, B.; Wischerhoff, E.; Arys, X.; Jonas, A.; Kauranen, M.; Persoons, A. *Angew Chem., Int. Ed. Engl.* **1997**, *36*, 2788−2791.

(3) Liu, Y.; Bruening, M. L.; Bergbreiter, D. E.; Crooks, R. M. *Angew. Chem., Int. Ed. Engl.* **1997**, *36*, 2114−2116. Liu, Y.; Zhao, M.; Bergbreiter, D. E.; Crooks, R. M. *J. Am. Chem. Soc.* **1997**, *119*, 8720−8721.

(4) Zhao, B.; Brittain, W. J. *J. Am. Chem. Soc.* **1999**, *121*, 3557−3558.

(5) Jordan, R.; Ulman, A.; Kang, J. F.; Rafailovich, M. H.; Sokolov, J. *J. Am. Chem. Soc.* **1999**, *121*, 1016−1022.

(6) (a) Prucker, O.; Ruhe, J. *Langmuir* **1998**, *14*, 6893−6898. (b) Prucker, O.; Ruhe, J. *Macromolecules* **1998**, *31*, 592−601. (c) Peng, B.; Ruhe, J.; Johannsmann, D. *Adv. Mater.* **2000**, *12*, 821−825. (d) Sidorenko, A.; Minko, S.; Schenk-Meuser, K.; Duschner, H.; Stamm, M. *Langmuir* **1999**, *15*, 8349−8355. (e) Ruths, M.; Johannsmann, D.; Ruhe, J.; Knoll, W. *Macromolecules* **2000**, *33*, 3860−3870.

(7) (a) Huang, X.; Doneski, L. J.; Wirth, M. J. *Anal. Chem.* **1998**, *70*, 4023−4029. (b) Husseman, M.; Malmstro, E. E.; McNamara, M.; Mate, M.; Mecerreyes, D.; Benoit, D. G.; Hedrick, J. L.; Mansky, P.; Huang, E.; Russell, T. P.; Hawker, C. *Macromolecules* **1999**, *32*, 1424−1431.

(8) Russell, R. J.; Sirkar, K.; Pishko, M. V. *Langmuir* **2000**, *16*, 4052−4054.

(9) Kim, N. Y.; Jeon, N. L.; Choi, I. S.; Takami, S.; Harada, Y.; Finnie, K. R.; Girolami, G. S.; Nuzzo, R. G.; Whitesides, G. M.; Laibinis, P. E. *Macromolecules* **2000**, *33*, 2793−2795.

(10) Bain, C. D.; Troughton, E. B.; Tao, Y. T.; Evall, J.; Whitesides, G. M.; Nuzzo, R. G. *J. Am. Chem. Soc.* **1989**, *111*, 321−335.

(11) Bain, C. D.; Evall, J.; Whitesides, G. M. *J. Am. Chem. Soc.* **1989**, *111*, 7155−7164. Laibinis, P. E.; Whitesides, G. M. *J. Am. Chem. Soc.* **1992**, *114*, 1990−1995. Laibinis, P. E.; Nuzzo, R. G.; Whitesides, G. M. *J. Phys. Chem.* **1992**, *96*, 5097−5105. Folkers, J. P.; Laibinis, P. E.; Whitesides, G. M.; Deutch, J. *J. Phys. Chem.* **1994**, *98*, 563−571.

(12) Schoer, J. K.; Zamborini, F. P.; Crooks, R. M. *J. Phys. Chem.* **1996**, *100*, 11086−11091. Zamborini, F. P.; Crooks, R. M. *Langmuir* **1997**, *13*, 122−126.

(13) Mrksich, M.; Sigal, G. B.; Whitesides, G. M. *Langmuir* **1995**, *11*, 4383−4385. Kajikawa, K.; Hara, M.; Sasabe, H.; Knoll, W. *Jpn. J. Appl. Phys., Part 2: Lett.* **1997**, *36*, L1116−L1119.

(14) Xia, Y.; Whitesides, G. M. *Angew. Chem., Int. Ed. Engl.* **1998**, *37*, 551−575. Kane, R. S.; Takayama, S.; Ostuni, E.; Ingber, D. E.; Whitesides, G. M. *Biomaterials* **1999**, *20*, 2363−2376.

(15) Yang, Z.-P.; Belu, A.; Sugg, H.; Liebmann-Vinson, A.; Chilkoti, A. *Langmuir* **2000**, *16*, 7482−7492.

(16) Azzam, R. M. A.; Bashara, N. M. In *Ellipsometry and Polarized Light*; Elsevier Science Publishers: North-Holland, The Netherlands, 1977.

(17) Yang, Z.; Frey, F.; Oliver, T.; Chilkoti, A. *Langmuir* **2000**, *16*, 1751−1758.

(18) Seferis, J. C. In *Polymer Handbook*, 4th ed.; Brandrup, J., Immergut, E. H., Grulke, E. A., Eds.; John Wiley & Sons: New York, 1999; p VI/581.

(19) Adamczyk, M.; Fishpaugh, J. R.; Mattingly, P. G. *Tetrahedron Lett*. **1995**, *36*, 8345−8346. Kovacs, J.; Mayers, G. L.; Johnson, R. H.; Cover, R. E.; Ghatak, U. R. *J. Org. Chem*. **1970**, *35*, 1810−1815.
(20) Briggs, D. In *Surface Analysis of Polymers by XPS and Static SIMS*; Cambridge University Press: Cambridge, UK, 1998; p 34.
(21) Seah, M. P.; Dench, W. A. *Surf. Interface Anal*. **1979**, *1*, 2−11.
(22) Powell, C. J. *J. Electron Spectrosc. Relat. Phenom*. **1988**, *47*, 197−214.
(23) Roberts, R. F.; Allara, D. L.; Pryde, C. A.; Buchanan, N. E.; Hobbins, N. D. *Surf. Interface Anal*. **1980**, *2*, 5−10. Cadman, P.; Gossedge, G.; Scott, J. D. *J. Electron Spectrosc*. **1978**, *13*, 1−6.
(24) Beamson, G.; Briggs, D. In *High-Resolution XPS of Organic Polymers: The Scienta ESCA 300 Database*; Wiley: Chichester, 1992.
(25) Briggs, D. In *Surface Analysis of Polymers by XPS and Static SIMS*; Cambridge University Press: Cambridge, UK, 1998; p 47.
(26) Nordfors, D.; Nilsson, A.; Markensson, N.; Svensson, S.; Gelius, U.; Lunell, S. *J. Chem. Phys*. **1988**, *88*, 2630−2636. Beamson, G.; Briggs, D. *Mol. Phys*. **1992**, *76*, 919−936.
(27) Huang, W.; Skanth, G.; Baker, G. L.; Bruening, M. L. *Langmuir* **2001**, *17*, 1731−1736.
(28) Ratner, B. D. In *Biomaterials Science: An Introduction to Materials in Medicine*; Academic Press: San Diego, 1996.
(29) Davies, J. *Nanobiology* **1994**, *3*, 5−16. Green, R. J.; Frazier, R. A.; Shakesheff, K. M.; Davies, M. C.; Roberts, C. J.; Tendler, S. J. B. *Biomaterials* **2000**, *21*, 1823−1835. Fagerstam, L. In *Techniques in Protein Chemistry II*; Academic Press: New York, 1991; p 65. Vadgama, P.; Crump, P. W. *Analyst* **1992**, *117*, 1657−1670. Chaiken, I.; Rose, S.; Karlsson, R. *Anal. Biochem*. **1992**, *201*, 197−210. Homola, J.; Yee, S. S.; Gauglitz, G. *Sensor Actuat. B: Chem*. **1999**, *54*, 3−15. Myszka, D. G. *Curr. Opin. Biotechnol*. **1997**, *8*, 50−57.
(30) Pockrand, I. *Surf. Sci*. **1978**, *72*, 577. Raether, H. In *Surface Plasmons on Smooth and Rough Surfaces and on Gratings*; Springer-Verlag: Berlin, Germany; 1988; p 19.
(31) Green, R. J.; Davies, J.; Davies, M. C.; Roberts, C. J.; Tendler, S. J. B. *Biomaterials* **1997**, *18*, 405−413.
(32) In *BIAtechnology Handbook*; Pharmacia Biosensor AB: Uppsala, Sweden, 1994.
(33) Reiter, R.; Motschmann, H.; Orendi, H.; Nemetz, A.; Knoll, W. *Langmuir* **1992**, *8*, 1784−1788. Erman, M.; Theeten, J. B. *J. Appl. Phys*. **1986**, *60*, 859−873. Jin, G.; Jansson, R.; Arwin, H. *Rev. Sci. Instrum*. **1996**, *67*, 2930−2936.
(34) Lom, B.; Healy, K. E.; Hockberger, P. E. *J. Neurosci. Methods* **1993**, *50*, 385−397. Nicolau, D. V.; Taguchi, T.; Tanigawa, H.; Yoshikawa, S. *Biosens. Bioelectron*. **1996**, *11*, 1237−1252. Makholiso, S. A.; Giovangrandi, L.; Leonard, D.; Mathieu, H. J.; Illegems, M.; Aebischer, P.; *Biosens. Bioelectron*. **1998**, *13*, 1227−1235. Nicolau, D. V.; Taguchi, T.; Tanigawa, H.; Yoshikawa, S. *Biosens. Bioelectron*. **1999**, *14*, 317−325.
(35) Singhvi, R.; Kumar, A.; Lopez, G. P.; Stephanopoulos, G. P.; Wang, D. I. C.; Whitesides, G. M.; Ingber, D. E. *Science* **1994**, *264*, 696−698. Mrksich, M.; Chen, C. S.; Xia, Y.; Dike, L. E.; Ingber, D. E.; Whitesides, G. M. *Proc. Natl. Acad. Sci. U.S.A.* **1996**, *93*, 10775−10778. Chen, C. S.; Mrksich, M.; Huang, S.; Whitesides, G. M.; Ingber, D. E. *Science* **1997**, *276*, 1425−1428. Patel, N.; Bhandari, R.; Shakesheff, K. M.; Cannizzaro, S. M.; Davies, M. C.; Langer, R.; Roberts, C. J.; Tendler, S. J. B.; Williams, P. M. *J. Biomater. Sci. Polym. Ed*. **2000**, *11*, 319−331.
(36) Folch, A.; Toner, M. *Biotechnol. Prog*. **1998**, *14*, 388−392. Patel, N.; Padera, R.; Sanders, G. H. W.; Cannizzaro, S. M.; Davies, M. C.; Langer, R.; Roberts, C. J.; Tendler, S. J. B.; Williams, P. M.; Shakesheff, K. *FASEB J*. **1998**, *12*, 1447−1554.
(37) Takayama, S.; McDonald, J. C.; Ostuni, E.; Liang, M. N.; Kenis, P. J. A.; Ismagilov, R. F.; Whitesides, G. M. *Proc. Natl. Acad. Sci. U.S.A.* **1999**, *96*, 5545−5548.
(38) Ostuni, E.; Kane, R.; Chen, C. S.; Ingber, D. E.; Whitesides, G. M. *Langmuir* **2000**, *16*, 7811−7819. Folch, A.; Jo, B. H.; Hurtado, O.; Beebe, D. J.; Toner, M. *J. Biomed. Mater. Res.* **2000**, *52*, 346−353.
(39) Cooper, E.; Wiggs, R.; Hutt, D. A.; Parker, L.; Leggett, G. J.; Parker, T. L. *J. Mater. Chem*. **1997**, *7*, 435−441. Cooper, E.; Parker, L.; Scotchford, C. A.; Downes, S.; Leggett, G. J.; Parker, T. L. *J. Mater. Chem*. **2000**, *10*, 133−139.

MA002125U